Setting Behavior, Apatite-forming Ability, Mechanical strength of Polymethylmethacrylate Bone Cement through Bioactivity Modification of Phosphate Functional Groups Combined with Ca^{2+} Ions

Dingze Chuan[a] Ling Zhang[b] Chongyan Leng[a] Qinghua Chen[a] Toshiki Miyazaki[c] Jinkun Liu[a, *]

[a] Faculty of Materials Science and Technology, Kunming University of Science and Technology, Yunnan, 650093, China

[b]R&D Center of China Tabacco Yunnan Industrial Co., Ltd, Yunnan, 650202, China

[b] Graduate School of Life Science and Systems Engineering, Kyushu Institute of Technology, Kitakyushu-shi, 808-0196, Japan

Detailed Author Information:

Dingze Chuan (as First author)

Affiliations: Faculty of Materials Science and Technology, Kunming University of Science and Technology, China, **Postal address**: No. 68 Wenchang Road, 121 Street, Wuhua-district, Kunming, Yunnan Province, 650093, China. **Tel&Fax:** +8615770288263, **E-mail:** chuandingze@163.com

Lang Zhang

Affiliations: R&D Center of China Tabacco Yunnan Industrial Co., Ltd, China, **Postal address**: Hongjin Road No.181, Wuhua District, Kunming, Yunnan Province, 650202, China. **Tel&Fax:** +8618987783807, **E-mail:** zhang-874005@163.com

Chongyan Leng

Affiliations: Faculty of Materials Science and Technology, Kunming University of Science and Technology, China, **Postal address**: No. 68 Wenchang Road, 121 Street, Wuhua-district, Kunming, Yunnan Province, 650093, China. **Tel&Fax:** +8615825289818, **E-mail:** 1259485316@qq.com

Qinghua Chen

Affiliations: Faculty of Materials Science and Technology, Kunming University of Science and Technology, China, **Postal address**: No. 68 Wenchang Road, 121 Street, Wuhua-district, Kunming, Yunnan Province, 650093, China. **Tel&Fax:** +8613888013957, **E-mail:** chenqinghua_yn1@163.com

Toshiki Miyazaki

Affiliations: Graduate School of Life Science and Systems Engineering, Kyushu Institute of Technology, Japan, **Postal address**: Graduate School of Life Science and Systems Engineering, Kyushu Institute of Technology, 2-4, Hibikino, Wakamatsu-ku, Kitakyushu-shi, 808-0196, Japan. **Tel&FAX:** +81-93-695-6025, **E-mail:** tmiya@life.kyutech.ac.jp

Jinkun Liu (as * Corresponding author)

Affiliations: Faculty of Materials Science and Technology, Kunming University of Science and Technology, China, **Postal address**: No. 68 Wenchang Road, 121 Street, Wuhua-district, Yunnan Province, Kunming, 650093, China. **Tel&Fax:** +8618987584793, **E-mail:** bio-liujinkun@kust.edu.cn

Setting Behavior, Apatite-forming Ability, Mechanical strength of Polymethylmethacrylate Bone Cement through Bioactivity Modification of Phosphate Functional Groups Combined with Ca^{2+} Ions

Abstract

Bioactivity modification helps Polymethylmethacrylate (PMMA) bone cement to reinforce its interfacial adhesion to bone tissues through the chemical bonding of apatite. Since Si-OH groups combined with Ca^{2+} ions have succeeded in inducing apatite formation, more combinations of functional groups and active ions are being explored. In this study, Bis[2-(methacryloyloxy)ethyl] phosphate (B2meP) containing phosphate (=PO_4H) groups and $Ca(CH_3COO)_2$ supplying Ca^{2+} ion were adopted to investigate the feasibility of equipping PMMA bone cement with apatite-forming ability *in vitro*, more effects under designed contents on setting behavior, injectability, contact angle, cytotoxicity and mechanical strength were also investigated. Results showed B2meP copolymerized with MMA and became one section of PMMA chains, surface =PO_4H groups and released Ca^{2+} ions pushed spherical apatite individuals nucleating and agglomerating into layer horizontally, Increasing B2meP content lowered the contact angle and the peak temperature, enhanced the cell viability of MC3T3-E1, but prolonged apatite forming period. Injectability rates performed a similar trend to setting time. Lower adding content and deposited apatite layer contributed to reduce the strength loss in soaking. Taking biological performance and other properties into balance, cement added with B2meP of 10 wt% in MMA and $Ca(CH_3COO)_2$ of 20 wt% in PMMA performed better.

Key words: PMMA bone cement, Bioactivity modification, Surface =PO_4H functional groups, Apatite-forming *in vitro*; Setting behavior; Mechanical Strength

1. Introduction

Cement-type biomaterial of PMMA owns similar characteristic of the cements used in architecture, the transformation from soft paste to hardened cement during the polymerization of methylmethacrylate (MMA) helps to create the characteristic of coherent matrix and deformable capacity, which makes the cement easily to be filled into the complex space of body parts. Therefore, PMMA bone cement is widely employed as the ideal candidate for the treatment of spinal compression fractures or the fixation of joint prosthesis in orthopedic surgery [1,2]. Since successful application in clinic, the typical shortcomings of cement itself have been exposed, for example, aseptic loosening of the prostheses has been reported in certain cases due to the thermal necrosis of bone tissue [3], and it can be ascribed to the exothermic polymerization during cement setting. Volume shrinkage and residual stress

remaining in preparation stage aggravate the cracks formation and propagation [4], which has been devoted to the deterioration of mechanical properties, shortened cement serving period *in vivo* [5]. Not only to these, the mechanical interlocking to bone tissues leads PMMA bone cement performing poor adhesion [6], which will lower the long-term stability of artificial joint prosthesis, raise the potential risk of repetitive operations on patients [7].

Bioactivity, i.e. the bone-bonding ability, has been proved more feasible in strengthening the bonding at the interface of implants and bone tissues [8,9]. In the early implantation period, the chemical bonding instead of physical connection depends on bone-like apatite, it's a special reaction product of bioactive materials and body fluid, whose component and structure are similar to that of inorganic mineral phase in natural bone [10]. After that, the bone-like apatite layer starts to absorb biological moieties, promote the cellular activities including the colonization, proliferation and differentiation by osteoblast stem cells, finally forms new bone and achieves the bony adhesion on the implant surface [11]. To PMMA bonce cement, there are two mainstream modification designs in equipping apatite-forming ability. First one is that, incorporating bioactive materials such as bioceramics [12], bioglass [13], graphene (oxide)-based composites [14,15] into the powder phase to synthesize the composite-type cement, utilizing the bioactivity of additives themselves to induce apatite depositing on cement surface. Although the composite cements have shown a tight contact to living bone when implanted into body environment, there are still some shortcomings left in the modification scheme itself. Most notably, the bioactive particles inside cement matrix lose their original function, apatite deposition is only occurred on cement surface where the bioactive particles can be exposed to body fluids. Thus, to obtain massive apatite deposits for better affinity performance requires high content of the additive, which in turn lead to a worsening on the physical properties of PMMA bone cement [16]. Another modification design is inspired from the apatite nucleation mechanism on bioglass45S5 reproduced in simulated body fluid (SBF). Si-O-Na components released the Na^+ ions to form Si-OH group via ion exchange with H_3O^+, the Si-OH functional groups owns the potential to attract Ca^{2+}, HPO_4^{2-} and OH^- ions gathering on surface, and released Na^+ ions increases the ionic activity product (IAP), both contributes to the nucleation of apatite [17]. Besides that, more groups like Ti-OH, Ta-OH, -COOH have been discovered to share the same role as Si-OH group [18-20], and the active ions for increasing IAP also expands to K^+ and Ca^{2+} ions [21,22]. Under this design thought, the most representative one was the combination of "Si-OH groups and Ca^{2+} ions", which succeeded in inducing apatite depositing on PMMA bone cement, the growth of new bone was also observed on the tibia of Japanese rabbit [23]. Besides that, the combination applied on commercialized Zimmers® dough-type cement also received higher osteoconductive properties through micro-CT

observation, the push-out load of 1.6 MPa indicated that modified specimens exhibited stronger bonding to bone tissues [24].

Except Si-OH groups, the phosphate groups self-assembled on Au substrate performed superior performance in inducing apatite deposition [25], being suggested as the next promising candidate for bioactivity modification. In this study, the BisP[2-(methacryloyloxy)ethyl] phosphate (B2meP) monomer whose chemical structure shown in **Figure 1** is added into the MMA, which is expected to be polymerized into PMMA main chain to increase the existence of $=PO_4H$ groups on cement surface. Calcium acetate powder is added into the PMMA to control Ca^{2+} releasing. The purpose is to equip PMMA bone cement with apatite-forming ability under the combination of $=PO_4H$ functional groups and Ca^{2+} ions, illustration about the role of additives on inducing apatite nucleation is shown in **Scheme 1**. And the study also put emphasis on investigating the effort brought by B2meP content on the setting behavior, apatite formation, cytotoxicity and mechanical strength, and final the additive content optimization will also be determined based on the balance of in vitro biological performance and standards in potential application.

2. Materials and Methods

2.1 Materials

PMMA beads was a commercial product brought from Sekisui Chemical Group (Tokyo, Japan), its molecular weights in Mw and Mm were 70,000 and 56,000, respectively, and the particle size was in a range of average size of 8.0~31.0 um. Benzoyl peroxide (BPO), Methylmethacrylate (MMA), N,N-dimethyl-p-toluidine (DmpT) and Calcium Acetate ($Ca(CH_3COO)_2{\cdot}H_2O$) were purchased from Wako Regent Company (Tokyo, Japan), Bis [2-(methacryloyloxy)ethyl] phosphate (B2meP) was ordered from Aladdin Regent Company (Kyoto, Japan). Calcium Acetate for cement modification need to be pretreated with the process of desiccating $Ca(CH_3COO)_2{\cdot}H_2O$ at 220 ºC for 2 h then passing through the 44 μm mesh sieve. Simulated body fluid (SBF) was prepared following reported protocol [26]. Mouse embryo osteoblast precursor (MC3T3-E1) cells were sourced from the Cell Bank of Chinese Academy of Sciences in Kunming, Dulbecco's Modified Eagle's Medium with high glucose (DMEM), Fetal Bovine Serum (FBS), penicillin/streptomycin solution, sterile Phosphate Buffered Saline (PBS) and Cell Counting Kit-8 (CCK-8) were purchased from Gibco Life Technologies (Green Island, NY, USA), NaOH and NaCl were offered by Sinopharm Chemical Reagent Co., Ltd (Shanghai, China).

2.2 Cement preparation

Components for PMMA bone cement modification were divided into 2 parts. To powder phase, PMMA beads were blended with pretreated $Ca(CH_3COO)_2$ and benzoyl peroxide (BPO) as the polymerization initiator. To liquid side, a mixture was composed of MMA, Bis [2-(methacryloyloxy)ethyl] phosphate (B2meP) and N,N-dimethyl-p-toluidine (DmpT) as the polymerization accelerator. Detailed weight fraction and naming for the component is given in **Table 1**, the additives merely replaced PMMA beads or MMA monomer, the contents of BPO and DmpT stayed the same, and the sample "B2meP0 + CA0" as the reference copied the compositions of commercially available cement CMW® 1, Debuy Synthes Co. Ltd., England. The condition for cement preparation was controlled at 23±2 ºC with a relative humidity (R.H.) of 50%±10%, and the mixing ratio of powder phase to liquid side was 1: 0.5 (P/L, g/g).

2.3 Physical properties Measurement

2.3.1 Setting behavior

Setting behavior of cement was measured following the guidance of ISO5833-2002 [27]. For the testing, a K-type thermocouple probe (Plamic 100Ω) coupled with a counting-type thermometer (DT-3891G, CEM-instruments Ltd., Shenzhen, China) was adopted to monitor and record the temperature rising in polymerization exothermic process, and the data logging interval was set as per second. Measurement procedure could be briefly described as below: temperature recording began from the powder and liquid coming into contact. After turning into no sticky state, the cement was filled into a cylindrical mold with the size of Φ 60×6 ±0.5 mm^2, and the K-type thermocouple probe was placed to the centre of mold to sense the temperature on cement surface over setting, and the recording continued until shortly after the temperature started to fall. Peak temperature was defined the maximum temperature over the setting process, and setting temperature was calculated by as the following formula:

$$\textit{Setting Temp.} = \frac{1}{2}\left(\textit{Room Temp.} + \textit{Peak Temp.}\right) \quad \textbf{(2-1)}$$

While, setting time was determined as the value that corresponding to the setting temperature on the temperature-time curve, which could be deeply illustrated in **Figure 2**. In this study, 4 repetitive measurements were necessary for each cement combination.

2.3.2 Injectability

Injectability was performed on cement paste to test the feasibility used in syringe usage. 10 g of powder was mixed with 5 g of liquid for 30 second, as the mixture turned into paste, a 20 ml medical sterile syringe in the size of φ1.6 × 30 mm^2 was used to extract the paste into the chamber to verify its extractability. As another mixture with same components turned into

no-sticky dough, it was plugged into chamber then extruded out to verify the injectability. Injectability rate to each combination was based on 3 repeated tests, and calculated as follow:

$$\textit{Injectability rate (\%)} = \frac{\textit{cement weight extruded from the syringe}}{\textit{cement total weight}} \times 100 \quad \textbf{(2-2)}$$

2.3.3 Contact angle

Contact angle measurement was performed on a professional meter (JC2000C, POWEREACH, Shanghai, China). Simulated body fluid (SBF) was chosen as the contact medium, PMMA bone cement for the measurement was molded into the rectangular sheet of $10 \times 15 \times 1 \pm 0.1$ mm^3 and polished by 1000# SiC paper at first. Measurement process could be briefly described as following: the SBF droplet was taken into photo as naturally dropping down to cement surface for 10 second, the contact angle was determined based on the shape of droplet in photo using goniometry method. To each sample, three different locations were selected.

2.3.4 Mechanical strength

Compressive strength measurement was following the requirements of ISO standard 5833 [27], and it was carried out on the Universal Testing Machine (Autograph AG-1, Shimadzu Co., Kyoto, Japan). Testing samples were shaped into the cylinder of $\phi 6 \times 12 \pm 0.1$ mm^2. In measurement, A 10 KN of compressive load with a crosshead speed of 20 mm/min was continuously pressed against the sample until the fracture happened, compressive strength was determined using the calculation expression below:

$$\delta_C = \frac{F}{A} = \frac{4 \times F}{\pi \times d^2} \quad \textbf{(2-3)}$$

where, F was the fracture load, A was the initial cross-sectional area. 7 specimens were tested for each set of combination.

Bending strength was performed on the same machine using three-point test. Testing specimens were molded in a beam shape with size of $60 \times 5 \times 4 \pm 0.1$ mm^3, and the loading rate was set as 5 mm/min. In measurement, the load towards to down was pressed on the middle site of beam specimen until the specimen was broken. Bending strength was calculated using the formula:

$$\delta_B = \frac{F}{A} = \frac{3 \times F \times L}{2 \times b \times h^2} \quad \textbf{(2-4)}$$

where, F was the load that fracture happened on the load–displacement curve, L was 40 mm in this study, representing the distance between two end supports. b and h were the width

and the height of beam specimen, respectively. And each cement formulation was carried on 5 times of duplication tests.

2.4 *In vitro* biological performance assay

2.4.1 Cytotoxicity

CCK-8 assay was carried out to determine in vitro cytotoxicity of PMMA bone cements through culturing of MC3T3-E1 cells with extracts of cements. The extract preparation needed cements being shaped into the ϕ 6×4 ±0.1 mm^2 disks in advance. All the disk samples were pre-treated with 75% ethanol and PBS for at least 12 h, respectively, subsequently immersed into 0.43 ml complete medium according to the cement/medium ratio of 3 cm^2/ml, the complete medium contained 89 vol% of DMEM, 10 vol% of FBS and 1 vol% of penicillin/streptomycin. After 24 h of immersion and filtration, the extract was ready to be used for the next co-culturing. MC3T3-E1 cells passaged to the 2nd generation were seeded in a 96-well plate at a cell density of 1×10^5 cells/cm^2, each well contained 100 μl of the complete medium. After 24 h incubation in a humidified atmosphere of 5% CO^2 at 37 ºC, the medium was removed and the extract was added, MC3T3-E1 cells continued to be incubated under the same condition for another 24 h. Then 10 μl CCK-8 reagent was added into each well and incubated additional 2 h, the 96-well plate was shifted to a microplate reader (Thermo Multiskan Spectrum, Thermo Scientific, USA) for measuring the absorbance of each well at 450 nm (OD450). Cell relative growth rate (RGR) was calculated by the formula below:

$$RGR = \frac{\left(OD_{TEST} - OD_B\right)}{\left(OD_C - OD_B\right)} \times 100\% \qquad \textbf{(2-5)}$$

While OD_C and OD_B represented the absorbance of control group and blank group, respectively. Cytotoxicity level of bone cements were given according to the judgment of ISO standard 10993 on RGR results [28].

2.4.2 Apatite forming ability in SBF

Whether PMMA bone cement equipping with apatite-forming ability was assessed in simulated body fluid (SBF), the ion concentration of SBF was of Na^+ 142.0, K^+ 5.0, Mg^{2+} 1.5, Ca^{2+} 2.5, Cl^- 147.8, HCO_3^- 4.2, HPO_4^{2-} 1.0 and SO_4^{2-} 0.5, mmol/L, nearly equal to that of human blood plasma. All cements shaped into the size of 10 × 15 × 1 ±0.1 mm^3 were polished with 1000# SiC paper in advance. Processed cements were soaked into sterile plastic bottles filled with 35 ml SBF, then placed in the condition of 37±1 ºC at the interval of 3, 7 and 14 days. After that, the specimens were removed, rinsed and dried at room temperature.

2.5 Characterization

Characterization of modified cements

Chemical structures of modified cements were characterized by FT-IR spectrometer (Tensor 27, Bruker Corporation, German) and ^{1}H-NMR (Bruker Avance 400, Bruker Corporation, German). FT-IR spectra was measured from the wavenumber of 400 cm^{-1} to 4000 cm^{-1} under the KBr pellet pressing method, the cements needed to be crushed into powders in advance. ^{1}H-NMR spectra were recorded at 400 Hz using $CDCl_3$ as the solvent.

Characterization of cements after SBF soaking

Thin-film X-ray diffractometer (MXP3V, MAC Science Ltd., Yokohama, Japan) and FT-IR spectrometer (FT/IR6100, Jasco Analytical Instruments, Tokyo, Japan) was employed to survey new phase on cement surface, TF-XRD pattern was scanned from 20º to 40º in 2θ under the scan rate of 0.02º/s, and the wavenumber in FT-IR spectra was set in a range of 500 cm^{-1} to 2000 cm^{-1}. Surface morphology of PMMA bone cements after SBF soaking were examined by SEM (S-3500N, Hitachi High-Technologies, Tokyo, Japan) combined with EDX microanalyzer (EMAX Energy, Horiba Ltd., Kyoto, Japan) after sputter coating a thin film of carbon on them. Concentration changes on the elements of Ca and P in SBF were measured by ICP-OES (Optima 4300 DV, PerkinElmer, Inc., America). And pH meter (F-23IIC, Horiba Ltd., Kyoto, Japan) was introduced to detect the pH value of cement-soaked SBF under the temperature of 37±1 ºC.

2.6 Statistical analysis

All results from repetitive experiments were expressed as mean ± standard deviation (SD). Statistical differences on means were analyzed by using one-way analysis of variance (ANOVA) with Turkey test method on SPSS 22.0, and the significance level was set as p value < 5%.

3. Results

3.1 Chemical structure analysis

FT-IR spectra of modified samples, CA powder and origin cement were shown in **Figure 3**. The absorbances at 1612 cm^{-1}, 1582 cm^{-1} were assigned to asymmetric stretching vibrations of COO^{-} groups, and absorbances at 1026 cm^{-1}, 952 cm^{-1}, 676 cm^{-1} were assigned to the stretching vibrations of C-O group, symmetric bending vibrations of $C\text{-}CH_3$ and bending vibrations of COO^{-} group, respectively. Those characteristic absorbances belonging to

$Ca(CH_3COO)_2$ were also detected on the spectra of "B2meP30 + CA 20" sample (comparison by blue dash line), and showed no obvious changes on wavenumbers, which reflected that CA powder indeed existed in cement matrix, but it was not involved in MMA polymerization to form chemical bonding with other components. Taking "B2meP0 + CA0" sample as the control, its absorbances and corresponding wavenumbers were almost same as those of sample "B2meP30 + CA0" and "B2meP30 + Ca20", which was speculated that B2meP was hard to be detected on FT-IR spectra, since B2meP and PMMA shared similar chemical groups, and the P-O stretching was hidden by peak overlapping. To further investigate whether B2meP additive in the PMMA matrix, ^{1}H-NMR spectra was employed and the comparison between "B2meP0 + CA0" and "B2meP30 + CA0" was shown in **Figure 4.** H signal (d) at the chemical shift of 4.2-4.4 was assigned as the group of $-(CH_2)_2-$ of B2meP, it was only detected on the sample of "b2meP30 + CA0", that proved that B2meP successfully copolymerized with MMA, and the copolymer of MMA-B2meP displayed the structure formula as speculated in **Scheme 1**. Moreover, the integral value of H signal from $-(CH_2)_2-$ group was 1.81 shown on the inset, while the H signal assigned to $C=CH_2$ groups owned integral values of 0.47 and 0.45 at the chemical shift of 6.1~6.15 and 5.55~5.60, respectively. The integral value for $-(CH_2)_2-$ groups from B2meP monomer was summed to 0.92. Difference of 0.89 (1.81-0.92) was attributed to the double bond of $C=CH_2$ from B2meP being engaged in polymerization reaction, further meant that over half of B2meP copolymerized with MMA, there was still unreacted MMA remained in cement matrix.

3.2 Setting behavior

Peak temperatures and setting times of cements modified with B2meP, CA or their combinations were listed in **Table 2**. It needed to be pointed that, no temperature rising was detected on the samples modified only with B2meP, the dough state was standing for at least 2 h. According to the definition of setting, these cements were categorized as unset cement, and required longer setting time. Compared to the reference sample of "B2meP0 + CA0", all the modified cements performed significantly lower peak temperature ($p<0.05$), and to the samples whose designed CA content was 20%, peak temperature showed a decline trend as increasing the content of B2meP, which contributed to preventing the thermal necrosis of bone tissue. Same comparison on the setting time, it was found that the additives and their combinations played more complicated roles, adding CA or B2meP alone significantly prolonged cement setting ($p<0.05$), considering the unset state was the extremity of setting time. While B2meP combined with CA made the setting of modified cements become significantly shortened ($p<0.05$), the fastest setting was detected on sample of "B2meP20+CA20", and any change on

B2meP content caused a prolonging of setting time. To clinical requirements of ISO standard 5833, the lower limit made two samples of “B2meP20+CA20” and “B2meP30+CA20” fail to satisfy the syringe usage.

3.3 Injectability

Injectability measurement was to verify whether bone cements after additives added could be used in syringe type, and the results were concluded in **Figure 5a,b** combined with **Table 3**. Photographs in **Figure 5b** showed all cement pastes were successfully extracted into chamber and extruded out, indicating that the modified cements still shared the same good extractability and extrudability as the reference sample of “B2meP0 + CA0”. And calculated injectability rates in **Table 3** revealed more details: only one additive either B2meP or CA, and B2meP10 combined with CA20 brought no obvious changes, the rest of cements performed significantly lower rates ($p<0.05$) compared with the original one, in which the lowest injectability rate of 74.28% ± 4.33% was detected on sample of “B2meP20 + CA20”. Injectability rate played a similar trend to that of the setting time, which implied there was a relationship between them.

3.4 Contact angle

Contact angle was one of the indicators in judging the hydrophilia of PMMA bone cement, **Table 4** listed the average values, which were measured based on the optical photos of SBF droplets shown in **Figure 6**. “B2meP0 + CA0” cement presented a contact angle of 74.5º ± 1.3º, below 90º meant PMMA bone cement itself was able to be wetted by SBF. No matter adding both or B2meP alone, the contact angles of modified cements were significantly reduced ($p<0.05$) via the comparison with reference sample. Among the cements added with both additives, “B2meP30 + CA20” sample showed the lowest contact angle of 45º ± 4.4º, while adding B2meP alone case put the highest adding content of 30 wt% owning the lowest contact angle of 15º ± 3.6º, two cases performed the same trend, the contact angle decreased with the increase of B2meP content, potentially implied that B2meP participated in the polymerization reaction and embedded into the main chain of PMMA, so that the hydrophilic $=PO_4H$ groups were resided on cement surface and helped to build better wettability. **Figure 6** is the visual images of SBF droplets on PMMA bone cement surface. The shape of droplet directly showed the variation trend of contact angle with the additive content. In addition, the difference on contact angle was also resulted from the droplets size, the evidence was discovered from the comparison of sample “B2meP0 + CA0” and “B2meP30 + CA0”.

3.5 *In vitro* cytotoxicity

Figure 7 reflects the effects of cement itself, additives and related adding amounts on in vitro toxicity of MC3T3-E1 cells. According to the standards of ISO 10993, the cell viability values were all beyond 80%, which demonstrated that all prepared cements were non-toxic, owned potential biological safety. The reference sample of "B2meP0 + CA0" performed a cell viability lower that 100%, the reason could be ascribed to the incompletely polymerized MMA, since its hazard had been proved to physiological environment [29]. As residual MMA was released from cement, its toxicity resulted in the cells hard to prolife in the extract. In contrast, all modified cements owns a significant higher cell viability that that of reference sample ($p<0.05$), which indicated that the additives and their combination played a positive role in promoting cell proliferation, and the positive role to cell viability became enhanced with increasing the content of B2meP, especially on the sample added with 20% or 30% of MMA, the cell proliferations showed a statistical significance ($p<0.05$) compared to other modified cements.

3.6 Induced apatite deposition

TF-XRD patterns of bone cements after soaking in SBF for the interval of 0, 3, 7, 14 days were displayed in **Figure 8.** From the patterns, Distinct diffraction peaks labeled with black-circle were appearing on the samples of "B2meP0 + CA20", "B2meP10 + CA20" and "B2meP20 + CA20". According to the identification of JCPDS Card no. 09-0432, these labeled peaks located at about 26º and 32º in 2θ were assigned as the (002) diffraction and an overlapping diffraction of (211), (112) and (300) of apatite, respectively, and lower intensity and wider peak shape indicated that deposited apatite was a lower crystallinity hydroxyapatite. More B2meP added in cement brought about the period postponement in first appearance of apatite, when B2meP adding amount reached to 30wt% of MMA liqiud, apatite deposition was extended to 14 days later due to no apatite peaks were detected. To the samples added with B2meP alone, 14 days soaking was unable to induce apatite depositing, which implied that merely relying on = PO_4H functional groups on bone cement surface were not sufficient to succeed in inducing apatite nucleation without additional Ca^{2+} sources.

To further figure out the morphology and constituents of deposited apatite, SEM combined with EDX were utilized, and the characterization results were shown in **Figure 9**. On the surface of "B2meP0 + CA20" sample, continuous nucleation of new apatite mainly occurred on the one had already deposited, which resulted in the deposits agglomerated to each other along longitudinal orientation, and performed a shape that close to the island. Apatite in island shape was similar the morphology that obtained from the cement incorporated with bio-ceramics like nano-HA [30]. Such morphology features further proved apatite deposition was

restricted to the sites where bioactive particles were liable to expose to SBF. While after another additive B2meP was added into cements, more apatite was nucleated in SBF soaking, and the quantity of deposits was increased with the adding content. Due to the heterogeneous nucleation brought by surface functional groups of $=PO_4H$, apatite deposits were relatively uniformly distributed on cement surface, and the agglomeration changed to horizontal direction, which led deposits to extending into the layer shape. On the magnified SEM images, it was clear to see that apatite individual was sphere-like, and the microsphere size appeared to be slightly decreased under the increase of apatite nucleation amount, apatite individual spheres owned a size range of 5~22 μm. EDX spectra showed that apatite deposits mainly contained Ca, P elements, and the calculated Ca/P atomic ratios on the corresponding modified cements were 1.60, 158 and 1.62, respectively. All ratios were lower than the stoichiometric ratio of 1.67 of $Ca_{10}(PO_4)_6(OH)_2$, apatite formed in SBF was judged as one sort of Ca-deficient hydroxyapatite [31], that was in accordance with the result concluded from the XRD patterns.

FT-IR spectra shown in **Figure 10a,b** was detected on cement surface before and after soaking, respectively, which was used to deeply exploring more detailed radical groups of modified cements and deposited apatite. Radical groups listed in **Table 5** were corresponding to those number-marked peaks appearing on the FT-IR spectra and considered to be the characteristics of PMMA. While the intrinsic peaks belonging to B2meP and $Ca(CH_3COO)_2$ were hard to be detected due to the overlapping of peaks. Comparison between **Figure 10a,b** manifested that, SBF soaking without apatite deposition never produced obvious changes on the FT-IR spectra, the new peaks marked with black triangle were identified as the typical P–O stretching, specifically including P-O ν4 vibration at 550 and 600 cm^{-1}, P-O ν1 vibration at 950 cm^{-1}, P-O ν3 vibration at 1020 cm^{-1} [32]. P–O peaks was derived from the deposited apatite through the confirmation from XRD patterns and SEM images. And the difference in FT-IR spectra on the samples of “B2meP0 + CA20”, “B2meP10 + CA20” and “B2meP20 + CA20” depended on the morphology of apatite shown in **Figure 9**, to “B2meP0 + CA20” cement, island shape apatite deposition caused cement surface remaining much of empty region, thus the FT-IR spectrometer was able to observe both PMMA and apatite. Once layered apatite covered on bone cement, there were only the characteristic peaks of apatite left, shown on the samples of “B2meP10 + CA20” and “B2meP20 + CA20”.

3.7 Ca, P concentrations changes in SBF

Concentration changes of Ca and P elements in SBF, corresponding pH values over the cement soaking time are displayed in **Figure 11a to 11c**, respectively. For Ca element shown in **Figure 11a**, its element concentration was an outcome of the dissolve-out amount of

$Ca(CH_3COO)_2$ deduct the consumption for apatite, the overall trend of Ca concentration was ascending with the extension of soaking period, higher concentration under the same soaking period was found on the sample with higher weight proportion of BisP, which implied that the loose matrix of PMMA bone cement changed by B2meP was liable to push more $Ca(CH_3COO)_2$ dissolution. For P element in **Figure 11b**, raising on its concentration was found on all $=PO_4H$ containing cements within 3 day of soaking, concentration rising was born of B2meP releasing, meant small part of B2meP was not involved in the polymerization reaction, while the next dropping of concentration on samples of "B2meP10 + CA20" and "B2meP20 + CA20"was resulted from the consumption for apatite nucleation, changes on P concentration over soaking period reflected whether there were apatite formation on cement surface, which was in accordance with the changes on TF-XRD patterns. Tendency of the pH variation of SBF was more complicated, the dissolution of alkaline $Ca(CH_3COO)_2$ and the release of acidic B2meP created the increase and the decrease of pH, respectively. Therefore, slight increase of pH on the samples of "B2meP0 + CA20" and "B2meP10 + CA20" implied that the effort produced by sufficient $Ca(CH_3COO)_2$ dissolution exceeded that brought by a small part of B2meP releasing. Continues dropping of pH was not only attributed to the consumption of OH^-, B2meP releasing under the high adding content became the main source and produced deeper dropping of pH, which was supported by the sample of "B2meP30 + CA20".

3.8 Mechanical performance

Figure 12a, b depicts the variations on compressive strength and bending strength of cements under additive contents and soaking periods, respectively. In **Figure 12a**, additives didn't bring a universal decline on the compressive strength to all modified cements before soaking, significant difference ($p<0.05$) was only detected on the sample whose B2meP content was increased to 30wt% of MMA, compared to the reference sample of "B2meP0 + CA0". After soaking, cements showed a lower compressive strength, but the decline in strength was not continued to the samples equipped with apatite-forming ability, compressive strength measured at 7 days and 14 days soaking were close to each other. Among all modified cements, the sample of "B2meP10 + CA20" owned the top average compressive strength, the detailed values were 97.7 ± 3.0 MPa and 98.4 ± 5.2 MPa under 7 days and 14 days soaking, respectively. In **Figure 12b**, bending strength displayed the variations similar to that of compressive strength: the decline still happened, but was not continued on the cements induced apatite forming. To the sample of "B2meP30 + CA20", B2meP content in 30wt% combined with 14 days soaking caused its bending strength failing to meet the lower limit of ISO 5833. In addition, "B2meP10 + CA20" sample still performed the top average bending strengths no matter being soaked for

7 days or 14 days. ANOVA analysis indicated that the top strengths either in compressive or in bending were significantly different from others, the differences might be produced by the lower adding amounts and the deposited apatite layer, according to the comparison and estimation based on the SEM images in **Figure 9** and the concentration changes in **Figure 11a,b**. In brief, although soaking caused the mechanical strengths of modified cements lower than those of the reference sample, but to the cements with apatite-forming ability, especially the sample of "B2meP10 + CA20", the strength values were beyond the lower limit of ISO 5833, which made them still own the qualification for clinical treatment.

4. Discussion

Setting, a polymerization process that liquid MMA was transformed into solid PMMA, relies on the benzoyl radicals and benzoyl anions, the decomposed products from a reduction-oxidation reaction between BPO and DmpT. Just like other additives of quaternized chitosan or bone marrow [33,34], $Ca(CH_3COO)_2$ was independent to the PMMA/MMA reaction system, their role in setting acted like barrier, which reduced the opportunity for contact between benzoyl radicals and MMA, further brought prolonged setting process due to the contact determined the broken of C=C double bond for initiating the formation of PMMA chains. Prolonged setting time was beneficial for the blood or fluid to carry more heat in advance through the cycle flowing, a lower exothermic temperature had been recorded when cement setting was measured at the human tibia *in vivo* [35]. Based on the reaction mechanism shown in **Figure 13**, since one by-product was H^+, the polymerization process was affected by the acidity of liquid phase. To most bioactive ceramics [13, 36], their neutral or alkalescent nature had almost no effect to the acidity of PMMA/MMA system, but the liquid B2meP monomer was more acidic, it brought higher acidity to the reaction system, and resulted in the oxidized benzyol radical was difficult to be converted into neutrality by proton separation, further extremely delayed the polymerization. When $Ca(CH_3COO)_2$ and B2meP were both added into PMMA cement, the alkalescence of $Ca(CH_3COO)_2$ could partly neutralize the acidity of B2meP and pushed the reaction system back to its normal pH range. In some sense, the neutralization meant both roles of $Ca(CH_3COO)_2$ and B2meP in prolonging the setting time were offset to each other, BPO/DmpT only served residual portion of PMMA/ MMA, therefore, setting time of modified cements became shortened. More about the negative role of B2meP could be further verified when the powder additive was changed as $Ca(OH)_2$. Except the influence of acidity of additive in reaction system, more mechanism should be clarified from the point that free electrons transfer on the benzoyl radicals and benzoyl anions [37,38].

To injectability, good extractability and extrudability of modified cements implied that the factors like designed amounts, CA powder size and B2meP monomer viscosity showed almost no efforts. More crucial role in determining the significant differences on injectability rates between cements was attributed to the setting time, since setting was a process of increasing the viscosity and decreasing the movability of cement paste [39]. Faster setting accelerated PMMA chains propagation and made part of cement paste remained into syringe chamber, which created an injectability rate trend similar to that of setting time.

Lower contact angle brought better hydrophila to cement, it conducted to improving the biological performance, especially in the deposition of apatite. Except the hydrophilic role of $=PO_4H$ functional groups on cement surface, the factors in decreasing the contact angle also included the cement setting behavior under additives. Poor cementation to the PMMA beads found on the unset samples, resulted in the intrinsically compact structure being worsened into loose, the loose structure coupled with the pores was liable to absorbed a part of the SBF droplet, which decreased the droplet size to make deeper contribution in reducing the contact angle. Adding more B2meP resulted to the decrease of the contact angle, while it supported to create a more suitable physiological environment for cell proliferation. Rising trend on the cell viability of MC3T3-E1 cells was attributed to the release of additives, noticeably occurred on the cement with more loose structure. In short, setting under the high content of B2meP and CA produced the loose structure on cement, which was beneficial to obtain better hydrophila and proliferation environment.

Although better hydrophila was beneficial for apatite deposition, SBF soaking results indicated that more about PMMA bone cement with apatite-forming ability was determined by the role of additive and related adding content. Inducing apatite nucleation was failed when cement was modified only with B2meP, one reason was speculated as dissociative Ca^{2+} ions in SBF was insufficient, they could not be transformed into precipitation under the attraction of $=PO_4H$ functional groups, increasing more Ca^{2+} ions on surface was able to be achieved by adding additional calcium source into cement, which was proved by the case of incorporating CA alone. Success in inducing apatite deposition on cement surface was attributed to the intrinsic characteristic of PMMA cement as a carrier used in antibiotics delivery [40], but the nucleation and growth was restricted to the location where $Ca(CH_3COO)_2$ particles were exposed to SBF. When both B2meP and CA were added, apatite morphology changed into the layer composed of individual microspheres, the coaction of Ca^{2+} ions and $=PO_4H$ functional groups in determining the generation of apatite layer was the same to the illustration shown in **Scheme 1**, Ca^{2+} ions supplied by high solubility (33.2g/100 ml in water at 40 ^oC) of

$Ca(CH_3COO)_2$ increased the supersaturation degree with respect to apatite, $=PO_4H$ groups on cement surface initiated the heterogeneous nucleation by evenly attracting Ca^{2+} ions. Unlike the reports that cements added with bioglass of SiO_2-Na_2O-CaO-P_2O_5-B_2O_3-Al_2O_3-Ag_2O or fluorapatite needed 28 days of soaking in inducing apatite deposition [41,42], the combination of B2meP and CA could shorten apatite forming period to 3 days. And a shorter biomineralization period was beneficial for lowering the response from immune system, especially in forming fibrous capsule and wrapping over the implant. It also contributed to prevent the wounds from stepping into the chronic inflammation stage, ensuring that bone trauma, defects and nonunion could be repaired and healed normally [43]. In addition, compared to the apatite agglomerating in longitudinal orientation, apatite horizontal spreading into layer fully covered in the gap between cement and bone tissues to form a whole connection on both sides, which was expected to further enhance the interface bonding *in vivo* at the early implantation stage.

B2meP was necessary to obtain apatite layer, but increasing its content also resulted in the postponement of apatite-forming period. According to the ionic activity product (IAP) of apatite in SBF [44] expressed below:

$$IAP = [Ca^{2+}]^{10}[PO_4^{3-}]^6[OH^-]^2\left(\gamma_{Ca^{2+}}\right)^{10}\left(\gamma_{PO_4^{3-}}\right)^6\left(\gamma_{OH^-}\right)^2 \quad \textbf{(4-1)}$$

where ***[]*** represented the activities of corresponding ions, and ***(γ)*** was the relative activity coefficients, usually identified as the empirical value of 0.36, 0.06 and 0.72 under the physiological environment, respectively.

Factors in determining the formation of apatite in this research were addressed as the concentrations of element Ca and P, and the pH of SBF (reflecting the concentration of OH^- ion). Concentration changes and pH trends over soaking in **Figure 11** indicated that, the activities of Ca^{2+} and PO_4^{3-} ions was enough even excessive, but sustained declined pH lowered the supersaturation degree of apatite, and bigger decline was following the increase of B2meP content, especially on the sample of "B2meP30 + CA20" at the 3rd day soaking . Rapid decline triggered by unreacted B2meP release made modified cement fail to induce apatite nucleation.

Enhanced mechanical strength of modified bone cement relied on additives, while CA in this study lacked of excellent mechanical performance like graphene (-oxide) or MWCNT [15,45], much less another B2meP was liquid organic monomer. According to published researches, reasons for strength loss of bone cement under bioactivity modification could be summarized into three categories: first one was the additives themselves, some of them were incapable to make up the strength loss from the replaced cement part [46]; the second was ascribed to the dissolution or release of additives, it produced pores in the matrix during

soaking, which brought a further worsen to strength [23]; and third one was pointed to the deposited apatite, once filling into the pores, it was able to alleviate the strength deterioration via preventing deeper loss of additives [47]. Back to compressive strength shown in **Figure 12a**, statistical difference between sample "B2meP0 + CA0" and "B2meP30 + CA20" indicated that B2meP content in the lower range of 0~20wt% didn't obviously brought obvious decrease on modified cements, More significant strength decline were detected on the same sample after SBF immersion. Therefore, the reason for strength loss in our study could be verified as the dissolution or release of CA and B2meP. Although soaking produced inevitable strength deterioration, there was still significant difference of strength on the bone cements equipped with apatite-forming ability. Difference on compressive or bending strength could be traced to the deposited apatite, especially to the morphology. Compared with island shape apatite, the layer apatite composed of spherical individuals owned a potential of alleviating the strength loss, its role was similar to the apatite filled into pores mentioned above, which was able to prevent the drain of additives.

Consequently, bioactivity modification under the combination of $=PO_4H$ functional groups and Ca^{2+} ions has successfully equipped PMMA bone cement with apatite-forming ability. The great advantage of combination modification is any materials containing functional groups or active ions can be selected as additives to explore the feasibility of inducing apatite nucleation, and there is no requirement that the additives themselves must be bioactive. Besides that, the addition of organic monomer in MMA is independent to that of calcium salt in PMMA powders, any changes of amounts on either side produced more combinations and variations on cement properties, especially for pushing mechanical modulus of modified cement close to the characteristic of bone. To satisfy the long-term stabilization of implantation, bioactivity modification on PMMA bone cement also needs to match the application standard of ISO 5833. Taking apatite-forming ability and clinical requirements into balance consideration, the additive contents of $Ca(CH_3COO)_2$ and B2meP in PMMA/MMA system were 20wt% and 10wt%, respectively. Modified bone cement is nontoxic, owns 314 s of setting time, 70.4 ^oC of peak temperature, 94.27% of injectability rate, 97.7 MPa of compressive strength and 59.1 MPa of bending strength after 14 days soaking, apatite layer composed of spherical individuals can be deposited within 3 days, shorter apatite-forming period is expected to play positive role in reinforcing the adhesion between cement and bone at the early implantation stage.

5. Conclusion

PMMA bone cements equipped with *in vitro* bioactivity in terms of inducing apatite deposition have been successfully developed under the combination of B2meP and

$Ca(CH_3COO)_2$. Coaction of phosphate (=PO_4H) functional groups and Ca^{2+} ions pushed the spherical apatite individuals horizontally spreading into layer, while increasing B2meP content brought the postponement to apatite forming period. Both additives lower the exothermic peak temperature and contact angle. Setting time performed the similar trend as injectability rates under the same additive contents. Cement strength depends on the additives contents and formed apatite morphology, lower adding content shows little loss of strength, and layered apatite is beneficial to alleviate the additive release over soaking. Comprehensive consideration based on all properties tells that, 10 wt% of B2meP and 20 wt% of $Ca(CH_3COO)_2$ have built PMMA bone cement with non-toxicity, apatite-forming ability, the setting behavior, injectability and mechanical strength satisfied for orthopedic application.

Acknowledgement

This work was supported by a Youth Project of Yunnan Applied Basic Research (Grant no. 2017FD096) and Yunnan Province Talent Cultivation Program (Grant no. KKSY201651024).

References

[1] Kühn KD. Bone cements: Up-To-Date Comparison of Physical and Chemical Properties of Commercial Materials, Heidelbelg(Berlin): Springer; 2011. P. 36–40

[2] Cisneros-Pineda OG, Cauich-Rodríguez JV, Cervantes-Uc JM, et al. Combined Influence of Barium Sulfate Content and Co-monomer Concentration on Properties of PMMA Bone Cements for Vertebroplasty. J Biomat Sci-Polym E. 2011;22(12):1563–1580.

[3] Do TJ. Polymethylmethacrylate: Properties and contemporary uses in orthopaedics. J Am Acad of Orthop Sur. 2010;18(5):297–305.

[4] Kinzl M, Boger A, Zysset PK, et al. The mechanical behavior of PMMA/bone specimens extracted from augmented vertebrae: A numerical study of interface properties, PMMA shrinkage and trabecular bone damage. J Biomech. 2012;45(8):1478–1484.

[5] Arora M, Chan EKS, Gupta S, et al. Polymethylmethacrylate bone cements and additives: a review of the literature. World J. Orthop. 2013;4(2):67–74.

[6] Skripitz R, Aspenberg P. Attachment of PMMA cement to bone: force measurements in rats. Biomaterials. 1999;20(4):351–356.

[7] Sylvain GM, Kassab S, Coutts R, et al. Early failure of a roughened surface, precoated femoral component in total hip arthroplasty. J. Arthroplasty. 2001;16(2):141–148.

[8] Nishiguchi S, Nakamura T, Kobayashi M, et al. The effect of heat treatment on bone-bonding ability of alkali-treated titanium. Biomaterials. 1999;20(5):491–500.

[9] Arcos D, Izquierdo-Barba I, Vallet-Regi M. Promising trends of bioceramics in the biomaterials

field. J Mater Sci: Mater Med. 2009;20(2):447–455.

[10] Kim HM, Kishimoto K, Miyaji F, et al. Composition and structure of the apatite formed on PET substrate in modified SBF with various ionic activity products. J Biomed Mater Res. 1999;46(2) 228–235.

[11] Hench LL, Thompson I. Twenty-first century challenges for biomaterials. J R Soc Interface. 2010;7(S4): S379–S391.

[12] Quan CY, Tang Y, Liu ZZ, et al. Effect of modification degree of nanohydroxyapatite on biocompatibility and mechanical property of injectable poly(methyl methacrylate)-based bone cement. J Biomed Mater Res B: Appl Biomater. 2016;104(3):576–584.

[13] Verné E, Bruno M, Miola M, et al. Composite bone cements loaded with a bioactive and ferrimagnetic glass-ceramic: Leaching, bioactivity and cytocompatibility. Mater Sci Eng C. 2015;53(1):95–103.

[14] Gonćalves G, Cruz SMA, Ramalho A, et al. Graphene Oxide versus functionalized carbon nanotubes as a reinforcing agent in a PMMA/HA bone cement. Nanoscale, 2012;4(9):2937–2945.

[15] Tavakoli M, Bakhtiari SSE, Karbasi S. Incorporation of chitosan/graphene oxide nanocomposite in to the PMMA bone cement: Physical, mechanical and biological evaluation. Int J Biol Macromol, 2020;149:783–793.

[16] Rentería-Zamarrón D, Cortés-Hernández DA, Bretado-Aragón L, et al. Mechanical properties and apatite-forming ability of PMMA bone cements. Mater Des. 2009;30(8):3318–3324.

[17] Kokubo T, Kim HM, Kawashita M, et al. Novel bioactive materials with different mechanical properties. Biomaterials. 2003;24(13):2161–2175.

[18] Uchida M, Kim HM, Kokubo T, et al. Apatite-forming ability of titania gels with different structures. J Biomed Mater Res A. 2003;64(1):164–170.

[19] Miyazaki T, Kim HM, Kokubo T, et al. Induction and acceleration of bonelike apatite formation on tantalum oxide gel in simulated body fluid. J Sol-gel Sci Technol. 2001;21:83–88.

[20] Sugino A, Miyazaki T, Ohtsuki C, et al. Apatite-forming ability of polyglutamic acid hydrogels in a body-simulating environment. J Mater Sci: Mater Med. 2008;19(6):2269–2274.

[21] Jeznach O, Gajc M, Korzeb K, et al. New calcium - free Na_2O – Al_2O_3 – P_2O_5 bioactive glasses with potential applications in bone tissue engineering. J Am Ceram Soc. 2018;101(2):602–611.

[22] Ohtsuki C, Kokubo T, Yamamuro T. Mechanism of apatite formation on CaO-SiO_2-P_2O_5 glasses in a simulated body fluid. J Non-cryst Solids. 1992;143:84–92.

[23] Miyazaki T, Ohtsuki C, Kyomoto M, et al. Bioactive PMMA bone cement prepared by modification with methacryloxypropyltrimethoxysilane and calcium chloride. J Biomed Mater Res A. 2003;67(4):1417–1423.

[24] Tsukeoka T, Suzuki M, Ohtsuki C, et al. Mechanical and histological evaluation of a PMMA-based bone cement modified with γ-methacryloxypropyltrimethoxysilane and calcium acetate. Biomaterials, 2006;21(21):3897–3903.

[25] Tanahashi M, Matsuda T. Surface functional group dependence on apatite formation on self-

assembled monolayers in a simulated body fluid. J Biomed Mater Res. 1997;34(3):305–315.

[26] Kokubo T, Takadama H. How useful is SBF in predicting in vivo bone bioactivity?. Biomaterials. 2006;27(15):2097–2915.

[27] ISO. “International standard 5833: Implants for surgery – Acrylic resin cements,” orthopaedic application, 2002(E).

[28] ISO. “International standard 10993-5: Biological evaluation of medical devices– Part 5: Tests for in vitro cytotoxicity,” orthopaedic application, 2009(E).

[29] Garza EG, Wadajkar A, Ahn C, et al. Cytotoxicity evaluation of methacrylate-based resins for clinical endodontics in vitro. J Oral Sci. 2012;54 (3):213–217.

[30] Che YL, Min S, Wang M.H., Biological activity of hydroxyapatite/poly(methylmethacrylate) bone cement with different surface morphologies and modifications for induced osteogenesis. J Appl Polym Sci. 2019;136(47):48188–48196.

[31] Lopes PP, Ferreirab Leite BJM, Almeida NAF, et al. Preparation and study of in vitro bioactivity of PMMA-co-EHA composites filled with a $Ca_3(PO_4)_2$-SiO_2-MgO glass. Mater Sci Eng C. 2008;28(4):572–577.

[32] Mohammadi Z, Mesgar A.S-M, Rasouli-Disfani F. Preparation and characterization of single phase, biphasic and triphasic calcium phosphate whisker-like fibers by homogenous precipitation using urea. Ceram Int. 2016;42(6):6955–6961.

[33] Tan HL, Guo SG, Yang SB, et al. Physical characterization and osteogenic activity of the quaternized chitosan-loaded PMMA bone cement. Acta Biomater. 2012;8(6):2166–2174.

[34] Arens D, Rothstock S, Windolf M, et al. Bone marrow modified acrylic bone cement for augmentation of osteoporotic cancellous bone. J Mech Behav Biomed. 2011;4(8):2081–2089.

[35] Biehl G, Harms J, Hanser U, Experimental studies on heat development in bone during polymerization of bone cement. Intraoperative measurement of temperature in normal blood circulation and in bloodlessness. Arch Orthop Unfallchir. 1974;78:62–69.

[36] Fukua C, Goto K, Imamura M, et al. Bone bonding ability and handling properties of a titania-polymethylmethacrylate (PMMA) composite bioactive bone cement modified with a unique PMMA powder. Acta Biomater. 2011, 7(10): 3595–3600.

[37] Cheng L, Weir MD, Zhang K, et al. Dental primer and adhesive containing a new antibacterial quaternary ammonium monomer dimethylaminododecyl methacrylate. J Dent. 2013;41(4):345–355.

[38] Macarie L, Ilia G. Poly(vinylphosphonic acid) and its derivatives. Prog Polym Sci. 2010;35(8):1078–1092.

[39] Kühn KD. Bone cements. Springer Publishing, Berlin, 2000;27-28.

[40] Russo T, Gloria A, Santis De R, et al. Preliminary focus on the mechanical and antibacterial activity of a PMMA-based bone cement loaded with gold nanoparticles. Bioactive Materials. 2017;2(3):156–161.

[41] Miola M, Bruno M, Maina G, et al. Antibiotic-free composite bone cements with antibacterial and

bioactive properties. A preliminary study. Mater Sci Eng C. 2014;43:65-75.

[42] Pahlevanzadeh F, Bakhsheshi-Rad HR, Hamzah E. In-vitro biocompatibility, bioactivity, and mechanical strength of PMMA-PCL polymer containing fluorapatite and graphene oxide bone cements. J Mech Behav Biomed. 2018;82:257–267.

[43] Siswomihardjo W. Biocompatibility Issues of Biomaterials. In: Mahyudin F., Hermawan H. (eds) Biomaterials and Medical Devices, Advanced Structured Materials. Springer Publishing, Berlin. 2016;41–65.

[44] Kim IY, Kikuta K, Ohtsuki C. Hydroxyapatite formation through dissolution-precipitation reaction: Effects of solubility of starting materials. Ceram Int. 2014;40(9A):14385–14390.

[45] Bakhtiari SSE, Karbasi S, Tabrizi SAH, et al. Evaluation of the effects of chitosan/multiwalled carbon nanotubes composite on physical, mechanical and biological properties of polymethyl methacrylate-based bone cements. Mater Technol. 2020;35(5):267-280.

[46] Boger A, Wheeler K, Montali A, NMP-modified PMMA bone cement with adapted mechanical and hardening properties for the use in cancellous bone augmentation. J Biomed Mater Res B. 2009;90(2):760–766.

[47] Sugino A, Miyazaki T, Kawachi G, et al. Relationship between apatite-forming ability and mechanical properties of bioactive PMMA-based bone cement modified with calcium salts and alkoxysilane. J Mater Sci Mater Med. 2008;19(3):1399–1405.

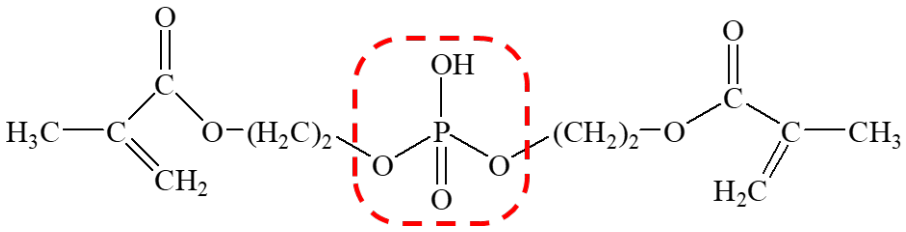

Figure 1. Chemical structure of Bis[2-(methacryloyloxy)ethyl] phosphate (B2meP)

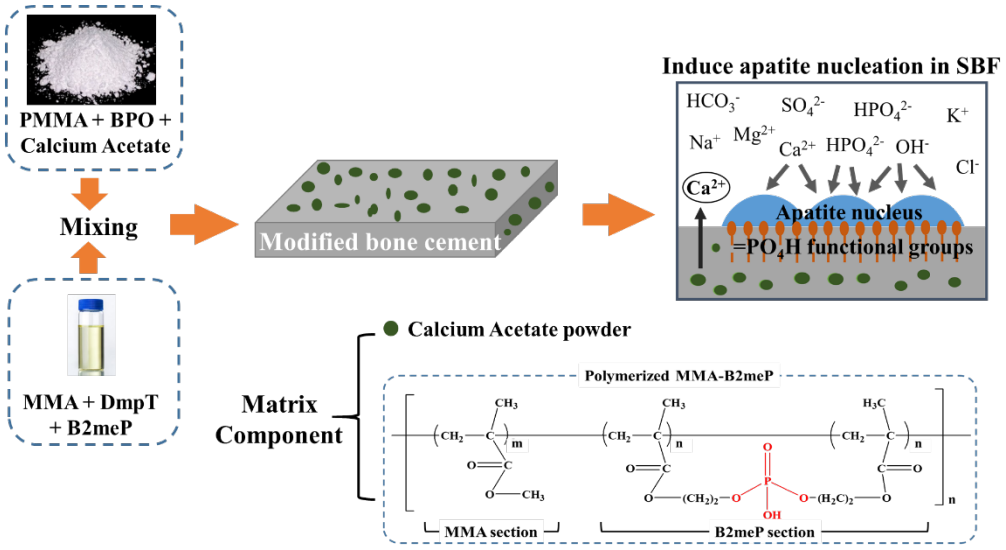

Scheme 1. Design of PMMA bone cement modified with B2meP and calcium acetate in inducing apatite nucleation

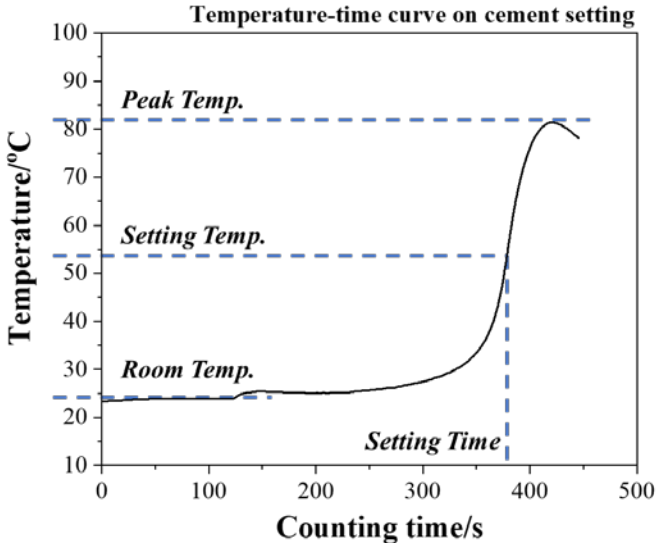

Figure 2. Typical temperature-time curve recorded on the cement setting process

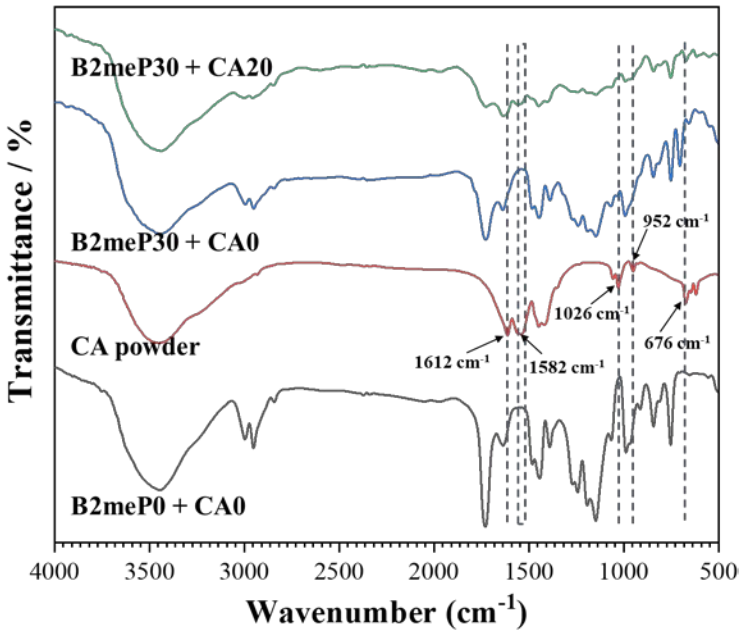

Figure 3. FT-IR spectra of modified cements, CA powder and reference sample as the controls

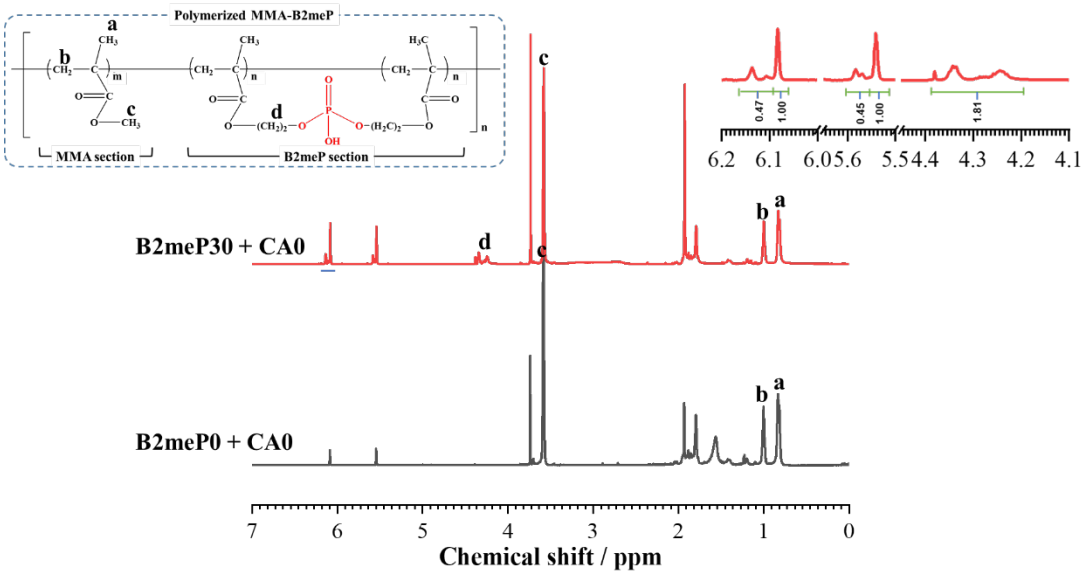

Figure 4. Comparison on the[1]H-NMR spectra of "B2meP0 + CA0" sample and "B2meP30 + CA0" sample

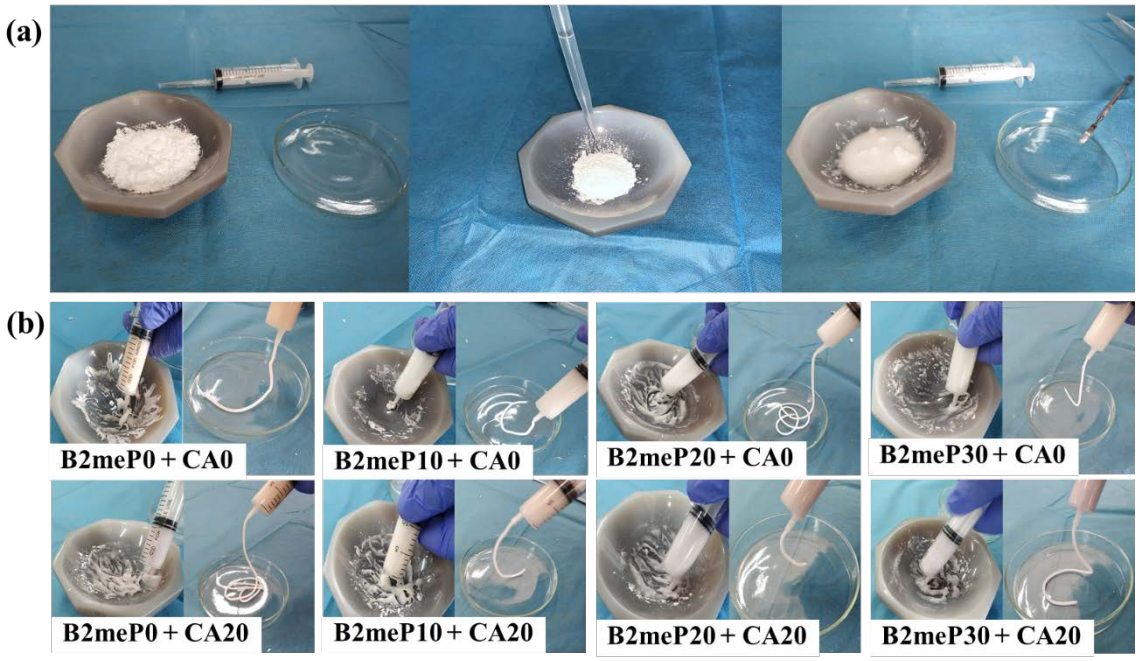

Figure 5. (a) powder, liquid and cement paste for injectability measurement from left to right; (b) Typical photographs of the extractability (left) and extrudability (right) of cements under designed combinations

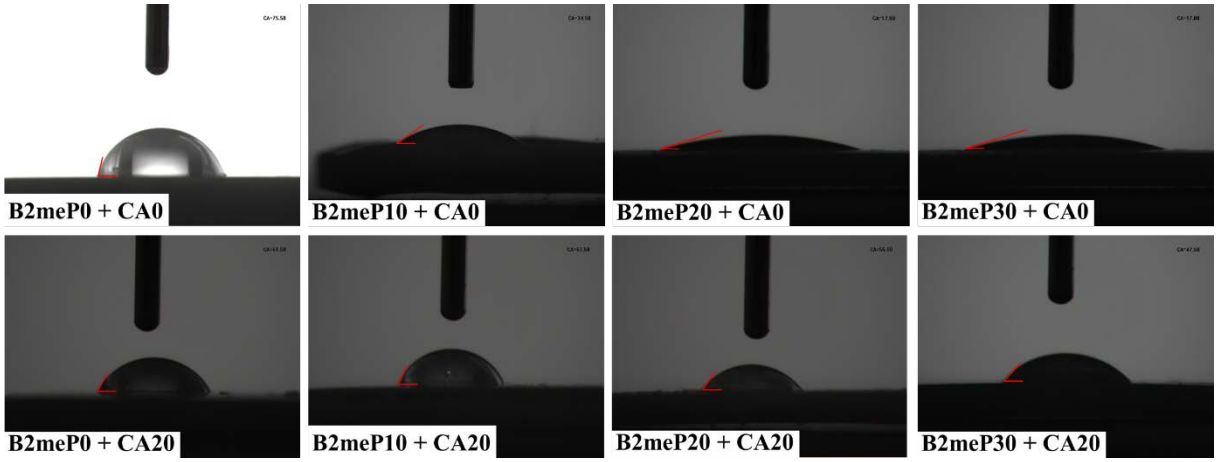

Figure 6. Typical optical photos of SBF droplet on cement surface captured after 10 seconds dropping

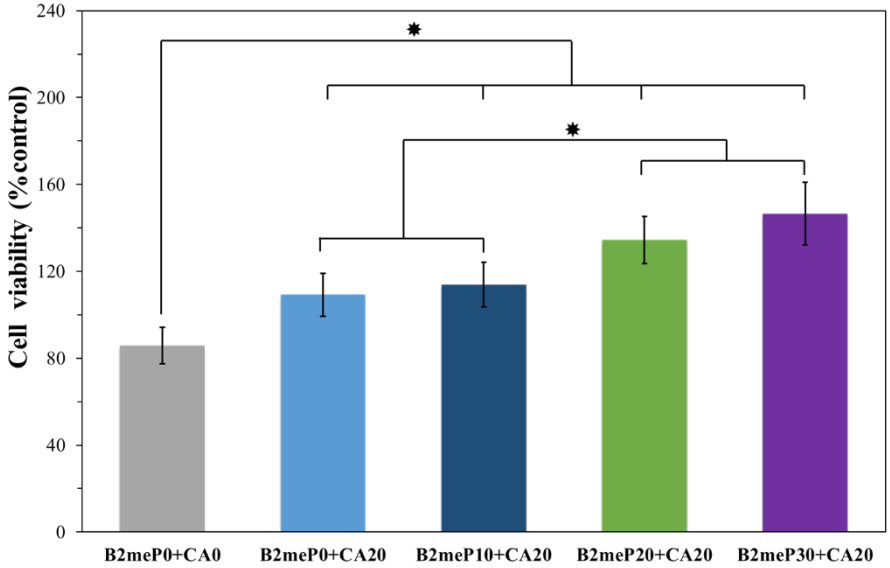

Figure 7. Cell viability of 2nd passage MC3T3-E1 cells after culturing in cement extracts for 24 h (✷: $p<0.05$)

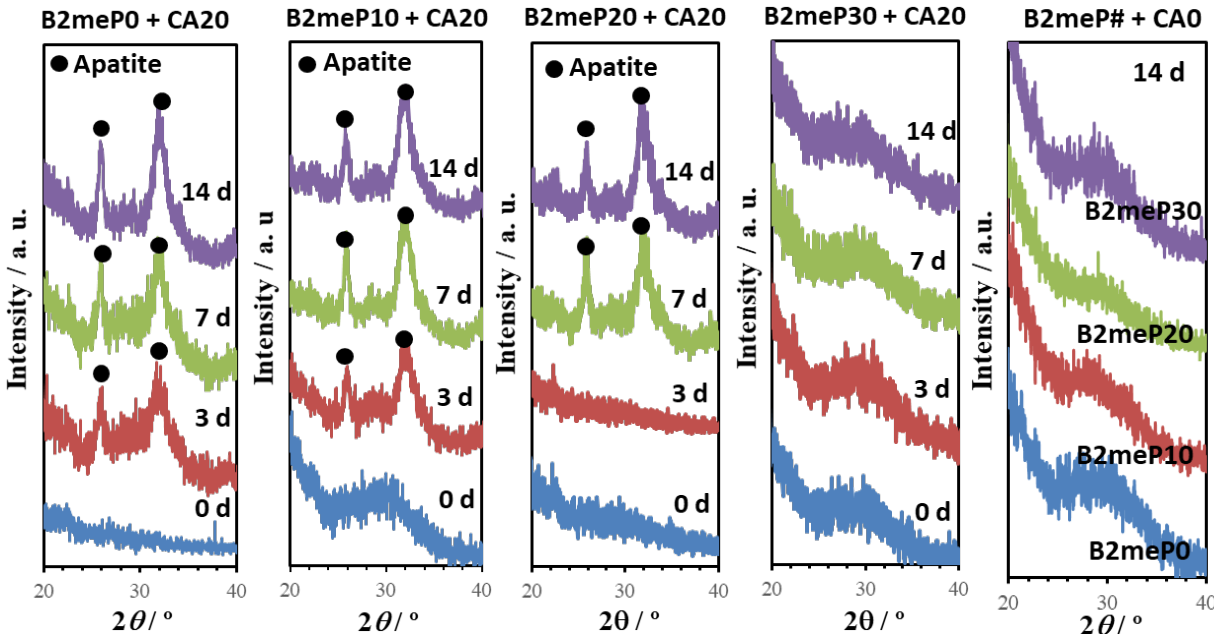

Figure 8. TF-XRD patterns on the surfaces of modified cements after SBF soaking

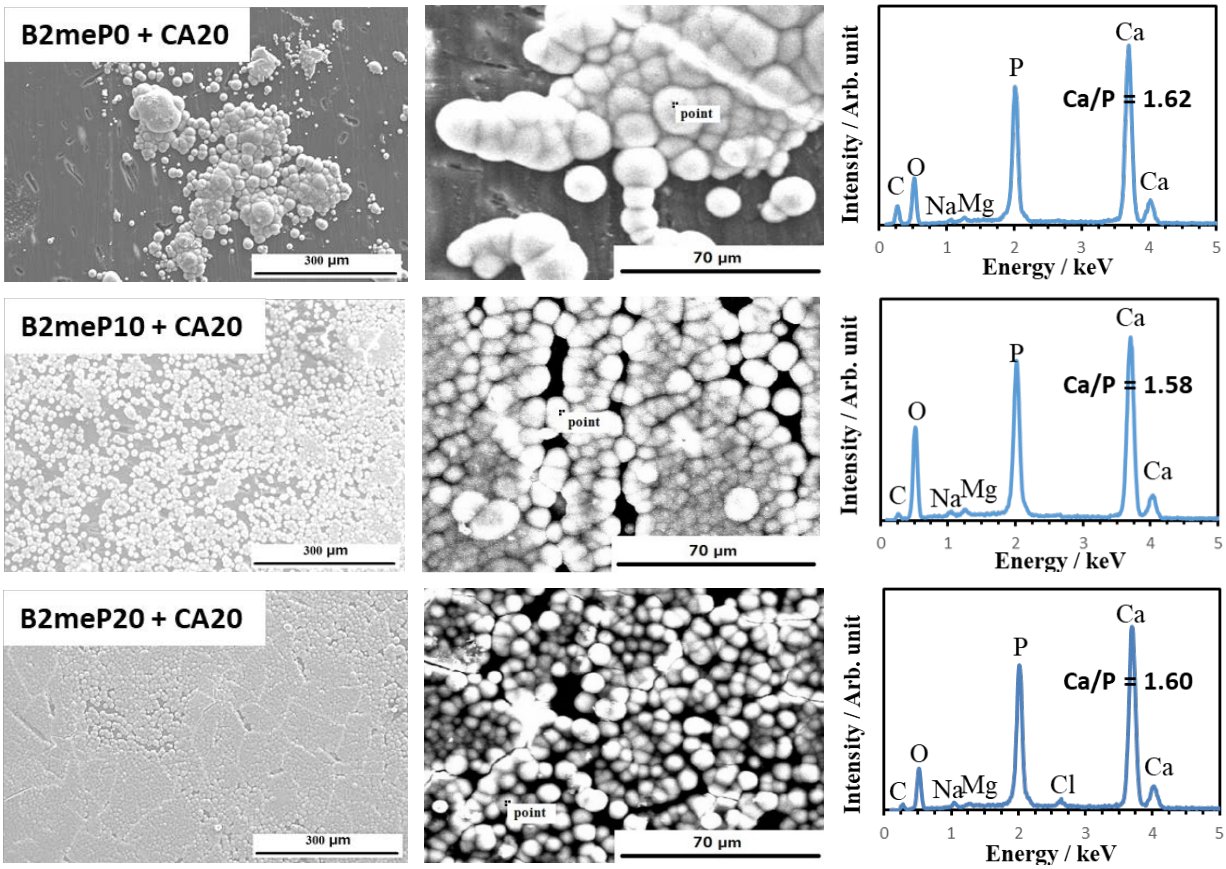

Figure 9. SEM images and EDX spectra of apatite deposited on modified cement surface

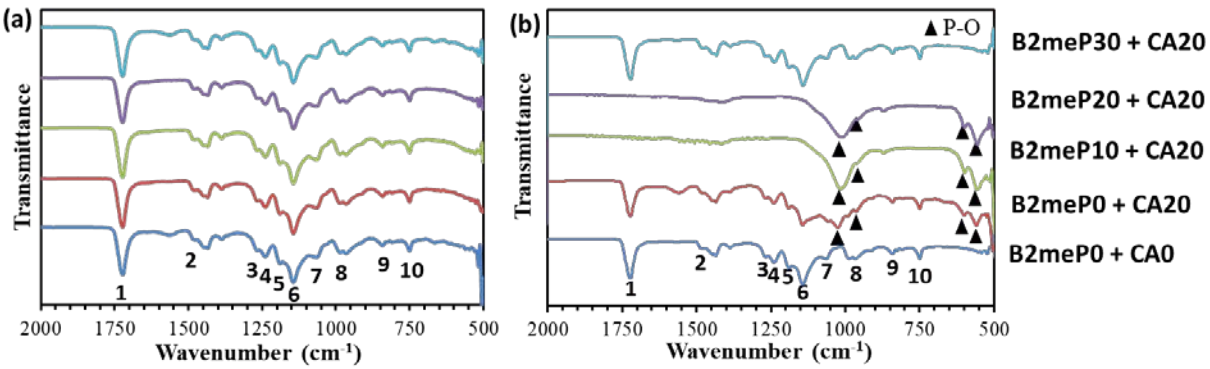

Figure 10. FT-IR spectra of the examined cements before (a) and after (b) soaking in SBF for 14 days

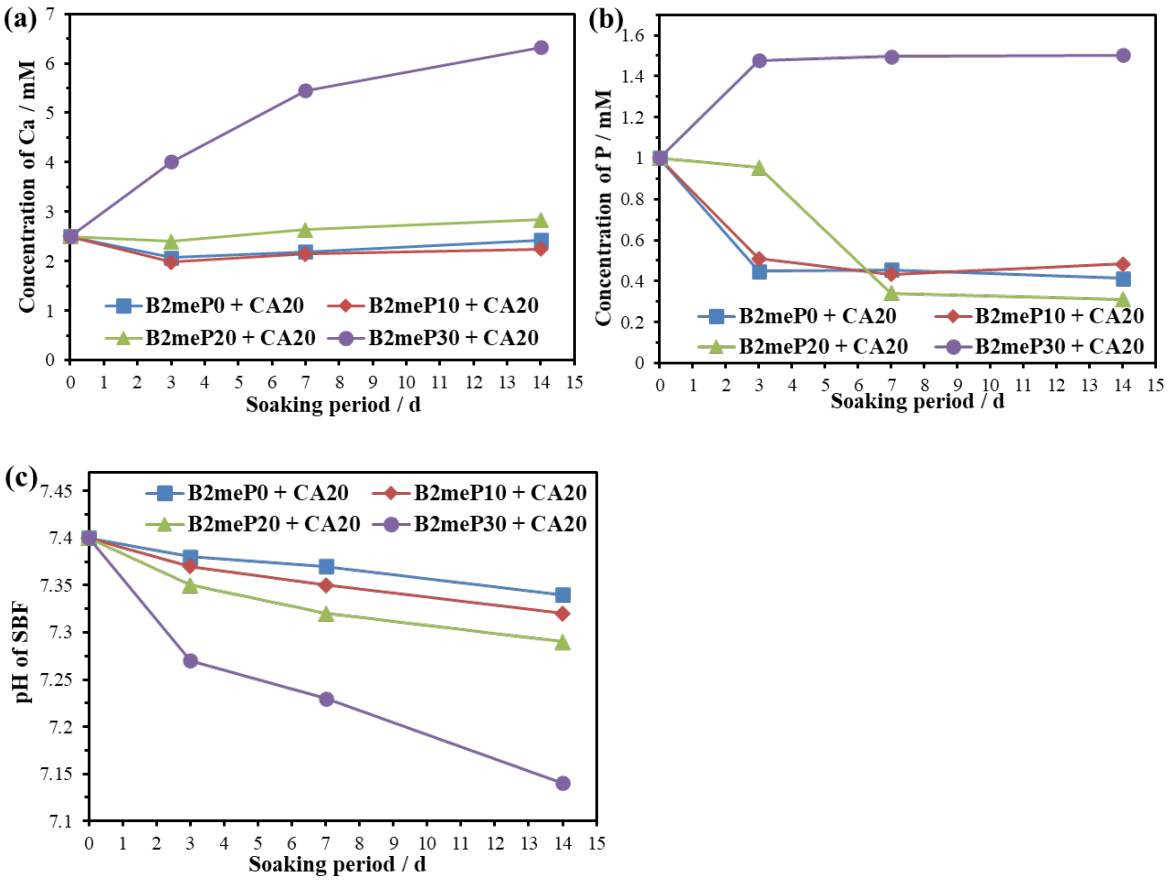

Figure 11. Concentration Changes of the Ca (a), P (b) elements in SBF and the pH variation (c) following sample soaking

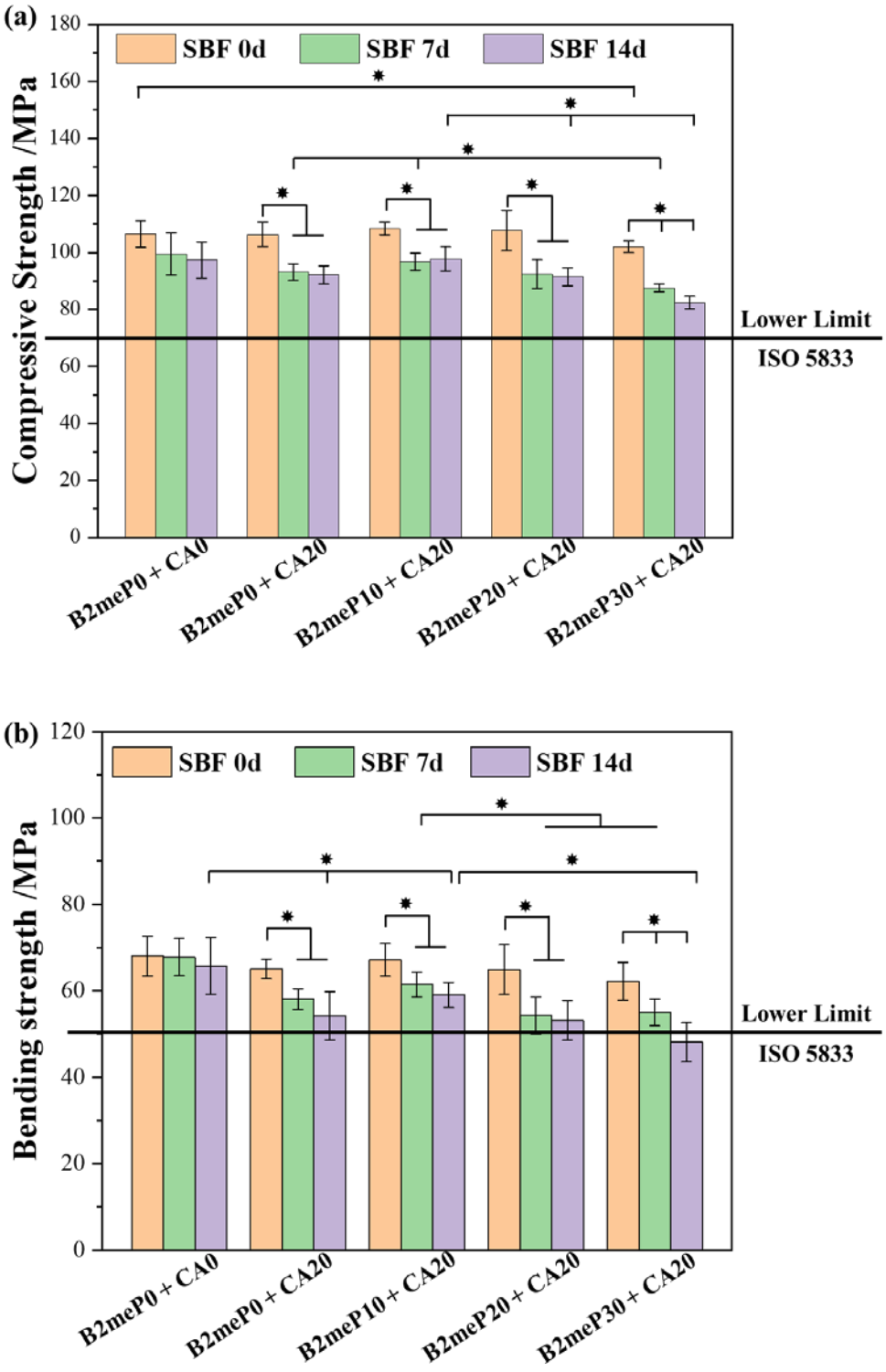

Figure 12. Variations on compressive strength (a) and bending strength (b) of bone cements under designed additive contents and soaking (✸: $p<0.05$)

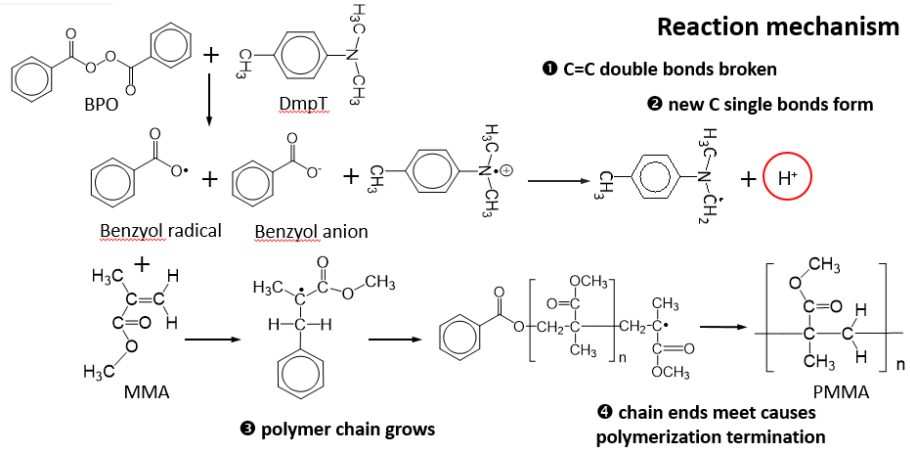

Figure 13. Polymerization reaction process of MMA into PMMA

Table 1. Detailed components of powder and liquid for examined combinations

CA#	Powder components (wt%)			B2meP#	Liquid components (wt%)		
	PMMA	BPO	CA		MMA	DmpT	B2meP
0	97.1	2.9	0	0	99.2	0.8	0
				10	89.2	0.8	9.93
20	77.7	2.9	19.4	20	79.4	0.8	19.8
				30	69.4	0.8	29.8

CA: pre-treated calcium acetate without crystal water, $Ca(CH_3COO)_2$.

Table 2. Setting behavior of examined cements based on the combinations

Setting Behavior		**Cement component**			
		B2meP0	B2meP10	B2meP20	B2meP30
Peak temperature (^oC)	CA0	82.3 ± 3.0	–	–	–
	CA20	76.5 ± 1.8[a]	70.4 ± 1.4[b]	68.9 ± 1.5[b]	63.5 ± 2.8[d]
Setting time (s)	CA0	361 ± 25	∞	∞	∞
	CA20	431 ± 29[a]	314 ± 4[b]	194 ± 11[c]	257 ± 9[d]

–: No rising in temperature, ∞: viewed as an unset cement;

[a]: Significantly different from B2meP0+CA0;

[b]: Significantly different from B2meP0;

[c]: Significantly different from B2meP0 and B2meP10;

[d]: Significantly different from B2meP0, B2meP10 and B2meP20;

Lower limit from ISO 5833: 180 s for dough state usage, 300 s for syringe usage

Table 3. Injectability rates of cements under designed additives contents

		Cement component			
		B2meP0	B2meP10	B2meP20	B2meP30
Injectability rate /%	CA0	96.82 ± 1.55	95.24 ± 1.54	96.23 ± 1.18	95.47 ± 0.73
	CA20	97.12 ± 1.18	94.27 ± 1.34[b]	74.28 ± 4.33[c]	85.37 ± 2.36[d]

[a]: Significantly different from B2meP0+CA0;

[b]: Significantly different from B2meP0+CA20;

[c]: Significantly different from B2meP0 and B2meP10;

[d]: Significantly different from B2meP0, B2meP10 and B2meP20;

Table 4. Contact angles of cements under designed contents of B2meP and CA

		Cement component			
		B2meP0	B2meP10	B2meP20	B2meP30
Contact Angle /^{o}	CA0	74.5 ± 1.3	32.3 ± 2.6 [b]	17.8 ± 1.7[c]	15 ± 3.6[c]
	CA20	64.8 ± 2.5[a]	62.8 ± 2.0[a]	56.1 ± 1.3[c]	45 ± 4.4[d]

[a]: Significantly different from B2meP0+CA0;

[b]: Significantly different from B2meP0;

[c]: Significantly different from B2meP0 and B2meP10;

[d]: Significantly different from B2meP0, B2meP10 and B2meP20;

Table 5. Radical groups presented in the spectra shown in Figure. 10

	Wavenumber (cm^{-1})	Combination	Functional groups
1	1723	C=O	Carbonyl C=O
2	1483	C-H	α-methyl (CH_3)
3	1280	C-H	α-methyl (CH_3)
4	1244	C-O	**-O-C**=O
5	1205	C-H	CH chains
6	1143	C-C	$C(CH_2)_n$ chains
7	1060	C-O	**-O-C**H_3
8	984	C=C	RH**C=C**H_2
9	843	C=O	R**C=O**OCH_3
10	752	C-H	-(CH_2)-